

PLASMA-PARTICLE INTERACTION EFFECTS IN INDUCTION

PLASMA MODELLING UNDER DENSE LOADING CONDITIONS

CONF-8307121--1

P. Proulx, J. Mostaghimi and M. Boulos

Department of Chemical Engineering

University of Sherbrooke

Sherbrooke, Québec, Canada J1K 2R1

DE84 013388

AC 02-77EV04320

ABSTRACT

The injection of solid particles or aerosol droplets in the fire-ball of an inductively coupled plasma can substantially perturb the plasma and even quench it under high loading conditions. This can be mainly attributed to the local cooling of the plasma by the particles or their vapour cloud, combined with the possible change of the thermodynamic and transport properties of the plasma in the presence of the particle vapour.

This paper reports the state-of-the art in the mathematical modelling of the induction plasma. A particle-in-cell model is used in order to combine the continuum approach for the calculation of the flow, temperature and concentration fields in the plasma, with the stochastic single particle approach, for the calculation of the particle trajectories and temperature histories. Results are given for an argon induction plasma under atmospheric pressure in which fine copper particles are centrally injected in the coil region of the discharge.

1. INTRODUCTION

Considerable effort has been devoted over the last ten years to the mathematical modelling of the inductively coupled plasma. This resulted in the development of a number of models which have become progressively more realistic and complex.

The first models by Mensing and Boedeker (1), Primore-Brown (2) and Eckert (3,4) were one-dimensional, aiming at the calculation of the radial temperature profile in the center of the coil by an energy balance between the local heat generation and heat losses by conduction and radiation.

The next generation of models were two-dimensional. The first of which were by Miller and Ayen (5) and Barnes et al (6-8) who took into account the effect of convective heat transfer in their calculation of the two-dimensional temperature field in the torch. This was followed by the work of Delettrez (9) and Boulos and his collaborators (10-13) who computed the two-dimensional temperature and flow fields in the plasma by solving the two-dimensional momentum and energy transfer equations simultaneously with the one-dimensional electric and magnetic field equations.

Attention was also given in the same time to the heating of particles as they are injected in the coil region of an induction plasma. Yoshida and Akashi (14) developed a numerical method for predicting the temperature

MASTER

history for a single iron particle injected along the centerline of an induction plasma. Boulos (15), reported results of computations of the two-dimensional trajectories and temperature histories of single alumina particles injected in the torch. The results revealed an important dependence of the particle trajectories and their temperature histories on the initial particle diameter, its initial radial position and injection velocity.

The approach used in either of these two investigations, however, involved the important assumption of negligible plasma-particle interaction. This assumption was necessary to decouple the particle trajectory and temperature history calculations from that of the plasma flow and temperature fields. A similar assumption was also made by other workers for the modelling of the thermal treatment of particles injected in d.c. plasma jet (16-17). While this assumption could be valid under low loading conditions when the number of particles, or the mass flow rate of the powder, injected in the plasma is extremely low, important interaction effects can be expected under most conditions used in the thermal treatment of powders in an induction plasma or in ICP spectrochemical analysis. With fine powder, the effect is stronger and more pronounced. This is because of the excessive vaporization which can affect the local energy distribution in the torch as well as the thermodynamic and transport properties of the plasma gas.

The present investigation aims specifically at the development of a mathematical model which could take into account the plasma-particle interaction effects in the computations of the two dimensional flow and temperature fields in an induction plasma. Obviously, if the effect of the particle vapours on the thermodynamic and transport properties of the plasma gas is also included, the model has to be extended to compute the two-dimensional concentration field of the particle-vapours in the plasma.

2. THE PROPOSED MODEL

The basic concept used to combine the continuum approach for the calculation of the flow, temperature and concentration fields in the plasma with the stochastic single-particle approach used for the calculation of the particle trajectories and temperature histories is the Particle-Source-In-Cell model (PSI-CELL) developed by Crowe and his collaborators (19) a few years ago for the analysis of a two-dimensional, spray-cooling problem.

According to this model, the energy and mass exchange between the particles and the fluid stream can be represented, as shown in figure 1, as individual source/sink terms in each of the finite-difference cells traversed by a particle during its trajectory in the flow. A flow chart of the overall computational scheme applied to our induction plasma modelling is given in figure 2. The approach used is essentially iterative with the source/sink terms in the energy and mass transfer equations continuously updated until a convergent flow and temperature field in the plasma is obtained. For simplicity, plasma-particle momentum transfer was not taken into account since it was in most cases negligibly small.

3. THE BASIC ASSUMPTIONS AND THE GOVERNING EQUATIONS

The basic assumptions involved in the modelling of the flow, temperature and concentration fields in the plasma were essentially similar to those used earlier by Boulos (10). The mathematical formulation, however, was modified adopting a new, and substantially more flexible and efficient, algorithm developed by Patankar (20) for the solution of the continuity, momentum,

energy and mass transfer equations written in terms of the velocity, pressure, enthalpy and concentration, respectively. Details of this new formulation adapted to induction plasma modelling are given in two recent studies by the present authors which are to be published shortly (12, 13).

Provision was made to include source/sink terms in the different equations to account for the plasma-particle interaction. This involved the addition of a local particle evaporation rate per unit volume \dot{m} to the continuity equation.

The momentum transfer equations were not affected since the particle-plasma momentum exchange was neglected in this stage of the work.

To the energy equation, a specific plasma-particle heat source-sink per unit volume, Q_{part} , was added. This consisted of two parts. The first represented the heat exchanged per unit volume between the plasma and the particles, while the second represents the heat per unit volume necessary to raise the temperature of the vapour evolved from the particles from their evaporation temperature to the temperature of the plasma.

As expected, the particle evaporation rate per unit volume, \dot{m} , was also included in the mass transfer equations as a source term.

In all of the gas-phase equations, the effect of the particle vapours on the thermodynamic and transport properties of the gas was taken into account.

3.2 Electric and magnetic field equations

These remained identical to those used earlier by Boulos (10-13).

3.3 Particle trajectory equations

These were also similar to equations used by Boulos (15) implying the assumptions of uniform particle temperature (21), no particle-particle interaction, particles not influenced by electromagnetic forces and negligible thermophoresis and Knudsen effects (22).

3.4 The source/sink terms

These were calculated by dividing the particle size distribution into, n_k , discrete sizes and assigning to each size fraction, n_k , different trajectories corresponding to different initial points of injection into the torch and different initial injection velocities. The number of particles per unit time injected along the trajectories crossing the (i,j) cell was then identified by N_{ij}^{kl} . The local number concentration of particles at any one time in the (i,j) cell is given by:

$$c_{ij}^{kl} = \frac{N_{ij}^{kl} \tau_{ij}^{kl}}{V_{i,j}} \quad . \quad 1.$$

where

τ_{ij}^{kl} is the residence time of the particles traveling along the kl trajectory in the i,j cell

$V_{i,j}$ is the volume of the i,j cell

for the continuity and the mass transfer equation the local source terms could then be calculated as:

$$\dot{m}_{ij} = \sum_{kl} c_{ij}^{kl} \frac{\Delta m_{ij}}{\tau_{ij}^{kl}} \quad 2.$$

where

Δm_{ij}^{kl} is the net change in the mass of the particles travelling along the trajectory (kl) during their residence in the cell (i,j)

for the energy equations the corresponding source/sink term can then be written as:

$$Q_{part,ij} = \sum_{kl} c_{ij}^{kl} (Q_{p,ij}^{kl} + Q_{v,ij}^{kl}) \quad 3.$$

where

$$Q_{p,ij}^{kl} = \frac{1}{\tau_{ij}^{kl}} \int_0^{\tau_{ij}^{kl}} h_c A_p (T - T_p) dt \quad 4.$$

$$Q_{v,ij}^{kl} = \frac{1}{\tau_{ij}^{kl}} \int_0^{\tau_{ij}^{kl}} \left(\frac{dm_{ij}}{dt} \right) c_{p,v} (T - T_p) dt \quad 5.$$

where h_c is the heat transfer coefficient between the particles and the plasma, A_p is the area of the particle, $C_{p,v}$ is the specific heat at constant pressure for the copper vapour.

4. RESULTS AND DISCUSSION

Computations were carried out for an induction torch of standard design. Details of the torch geometry, dimensions and operating conditions are given in figure 3. The torch was operated at atmospheric pressure with argon as the plasma gas. A fine copper powder was injected centrally in the discharge entrained by the gas stream Q_1 . The initial particle velocity was assumed to be that of the gas at the point of injection. The physical and thermodynamic properties used for the copper are given in Table 1. The thermodynamic and transport properties of the argon-copper vapour mixture under plasma conditions used were those reported by Mostaghimi (23).

Two copper powders were used with normal number particle size distributions. These had the same mean particle size of 70 μm but different standard deviations. One of the powders was assumed to have a wide distribution ($10 < d_p < 130 \mu\text{m}$) while the other has a substantially narrower distribution ($64 < d_p < 76 \mu\text{m}$). The total powder injection rate was varied between 1.5 and 12.0 g/min.

A summary of the results in Table 2 shows the overall copper evaporation rates under different conditions and the percentage of the plasma power (3 kW) which is used to heat up the particles and the generated copper vapour.

Typical results given in figure 4 show the temperature, flow and concentration fields in the torch with 7.5 g/min of copper powder ($10 < d_p < 130 \mu\text{m}$) injected in the discharge. It may be noted that due to the relatively high central injection, $Q_1 = 3.0 \text{ l/min}$, most of the copper particles assume an axial trajectory close to the axis of the torch. After an initial heat-up and melting period, the copper starts to evaporate close to the end of the coil region. This gives rise to the vapour cloud illustrated in figure

4-b by the concentration iso-contours. The absence of any copper vapour in the coil region (Energy Addition Region) is particularly relevant since it could have strongly influenced the overall temperature field in the torch through its effect on the electrical conductivity of the argon. The latter has been shown by Mostaghimi and Pfender (23) to increase by one order of magnitude at temperature lower than 8500 K in the presence 0.1% of copper vapour in the gas.

The local thermal loading effect on the plasma due to the injection of the copper powder in the discharge region is particularly evident in figure 5. Two points are to be noted from this figure. The first is that the cooling of the plasma is limited to the central region of the flow ($r < 5 \text{ mm}$). Secondly, while, as shown in Table 2, an increase of the powder feed rate from 1.5 to 12.0 g/min results in an increase of the percent of the plasma power absorbed by the powder from only 3.8 to 14.2%, the plasma temperature at the center of the coil drastically drops from 4200 K to close to 700 K. The effect also gives rise to an overall drop of the temperature profile along the axis of the torch as shown in figure 6. A similar, although smaller effect is noted on the axial velocity profile along the centerline of the torch as shown in figure 7.

ACKNOWLEDGMENT

This work was partially supported by the Department of Energy (Office of Basic Energy Sciences) through contract EE77-S-02-4320. The support by the Ministry of Education of the Province of Québec and the Natural Science and Engineering Research Council Canada is gratefully acknowledged.

REFERENCES

- (1) Mensing, A.E. and L.R. Boedeker, NASA, CR-1312 (1969).
- (2) Primore-Brown, D.C., J. Appl. Phys., 41, 3621 (1970).
- (3) Eckert, H.U., J. Appl. Phys., 41, 1529 (1970).
- (4) Eckert, H.U., J. Appl. Phys., 43, 46 (1972).
- (5) Miller, R.J. and J.R. Ayen, J. Appl. Phys., 40, 5260 (1969).
- (6) Barnes, R.M. and R.G. Schleicher, Spectrochim Acta, B-30, 109 (1975).
- (7) Barnes, R.M. and S. Nikdel, Appl. Spectrosc. 29, 477 (1975).
- (8) Barnes, R.M. and S. Nikdel, J. Appl. Phys., 47, 3929 (1976).
- (9) Delettrez, J.A., "A Numerical Calculation of the Flow and Electrical Characteristics of an Argon Induction Discharge", PhD Dissertation, U. of California, Davis (1974).
- (10) Boulos, M.I., IEEE, Trans. Plasma Sc., Ps-4, 28 (1976).
- (11) Boulos, M.I., R. Gagné and R.M. Barnes, CJChE, 58, 367 (1980).
- (12) Mostaghimi, J., P. Proulx and M.I. Boulos, to be published (1983).
- (13) Mostaghimi, J., P. Proulx and M.I. Boulos, to be published (1983).
- (14) Yoshida, T. and K. Akashi, J. Appl. Phys., 48, 2252 (1977).
- (15) Boulos, M.I., IEEE, Trans. Plasma Sc., PS-6, 93 (1978).
- (16) Boulos, M.I. and Gauvin, CJChE, 52, 355 (1974).
- (17) Fiszdon, J.K., Int. J. Heat Mass Transfer, 22, 749 (1979).
- (18) Vardelle, M., A. Vardelle, P. Fauchais and M.I. Boulos, AIChEJ, 29 (1983).
- (19) Crowe, C.T., M.P. Sharma, D.G. Stock, J. Fluids Eng., 325 (1977).
- (20) Patankar, S.V., "Numerical Heat Transfer and Fluid Flow", McGraw Hill (1980).
- (21) Bourdin, E., P. Fauchais and M.I. Boulos, I. J. Heat Mass Transfer, 26, 567 (1983).
- (22) Chen, X. E. Pfender, Plasma Ch. & Plasma Proc., 3, 97 (1983).
- (23) Mostaghimi, J. and E. Pfender, to be published (1983).

Table 1. Properties of Copper

| T_f [K] | T_e [K] | ΔH_f [KJ/Kg] | ΔH_e [KJ/Kg] | C_p [KJ/KgK] | $C_{p,vap}$ [KJ/KgK] | ρ [Kg/m ³] |
|--------------|--------------|-------------------------|-------------------------|-------------------|-------------------------|--------------------------------|
| 1356 | 2840 | 2×10^6 | 5×10^6 | 425 | 480 | 8900 |

Table 2. Summary of results for copper particles, $d_p = 70 \mu\text{m}$

| Particle size range [μm] | Powder feed rate m_p [g/min] | Powder evaporated m_v [g/min] | Power absorbed | | % of plasma power absorbed |
|--|--------------------------------------|---------------------------------------|----------------|--------------|----------------------------|
| | | | Q_p [W] | Q_v [W] | |
| 10-130 | 1.5 | 0.58 | 113 | 23 | 3.8 |
| " | 4.5 | 1.12 | 257 | 36 | 8.6 |
| " | 7.5 | 1.26 | 340 | 35 | 11.3 |
| " | 12.0 | 1.20 | 426 | 29 | 14.2 |
| 64-76 | 4.5 | 2.8 | 328 | 47 | 10.9 |

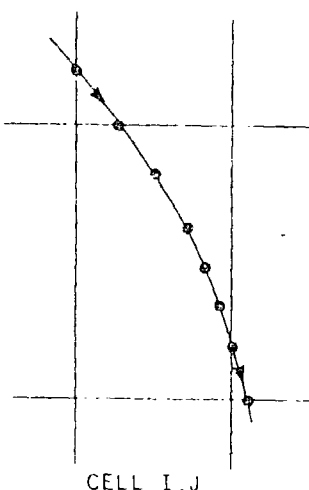


Figure 1. Schematic of an I,J Cell in the PSI-CELL Model

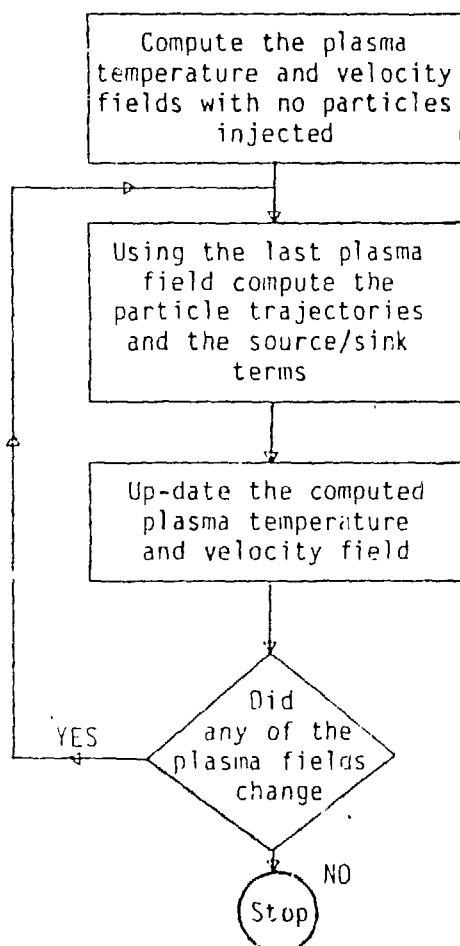


Figure 2. Flow chart of the proposed model including plasma-particle interaction effects

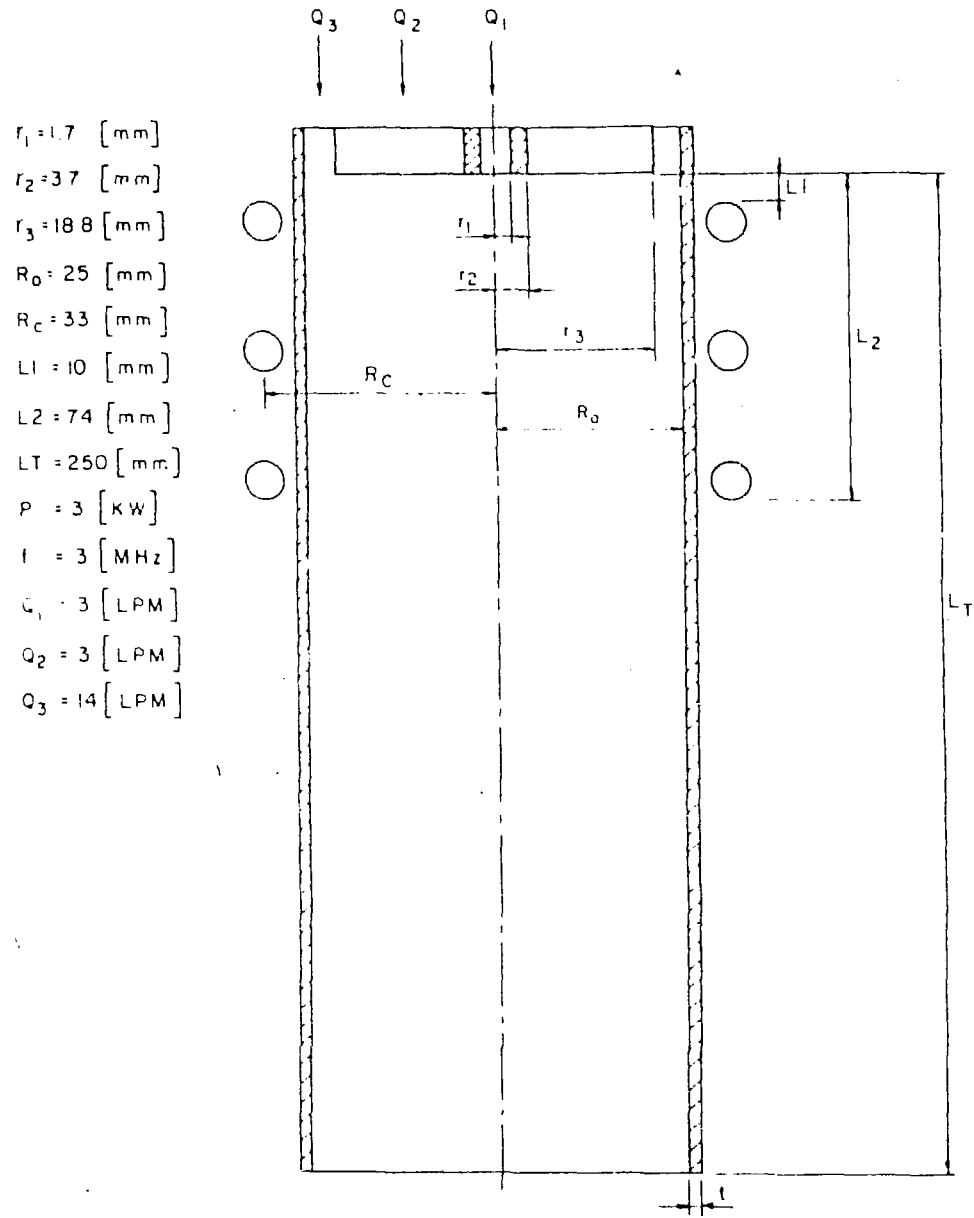


Figure 3. Torch geometry, system of coordinates and operating conditions

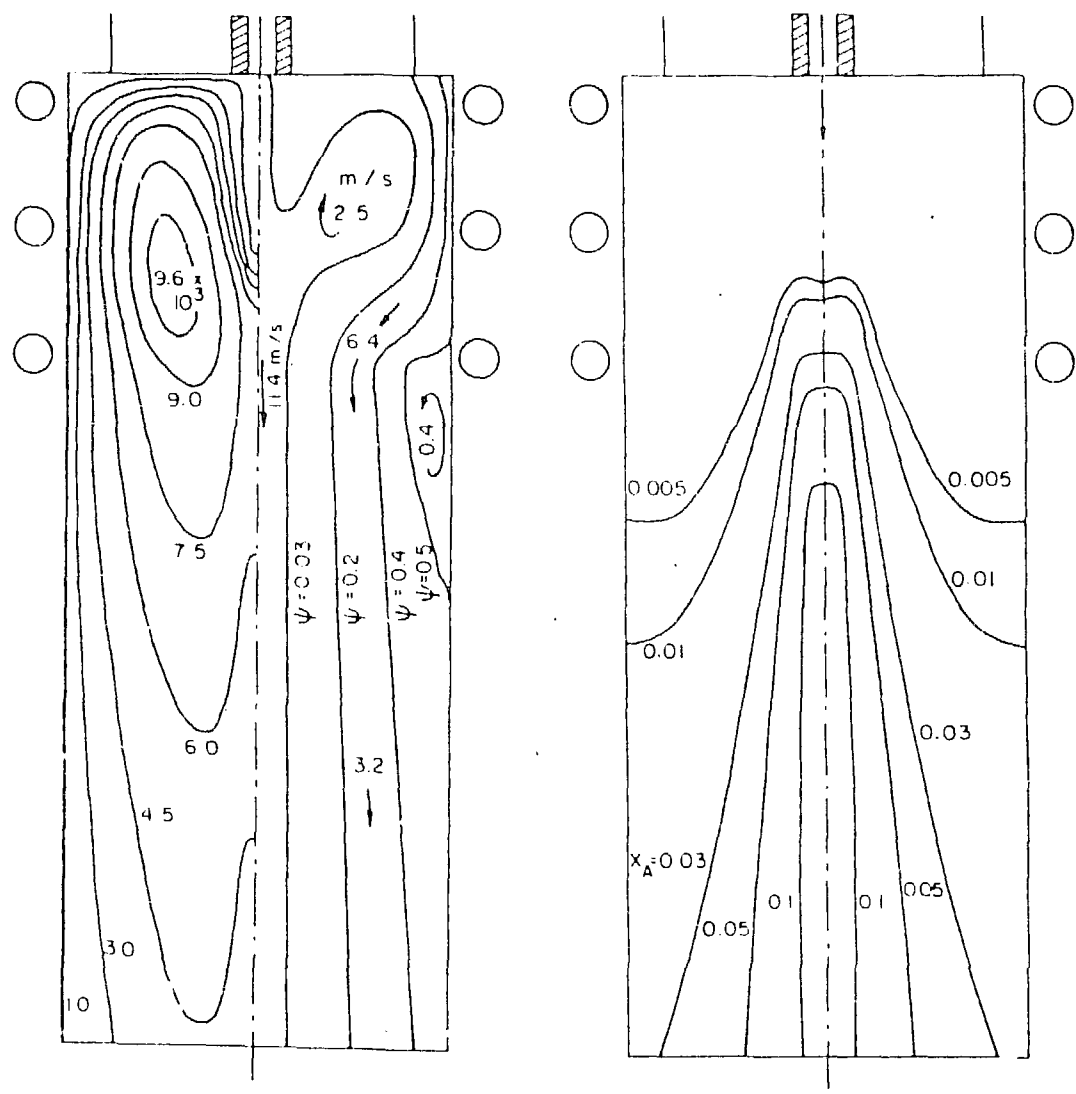


Figure 4. Temperature, flow and concentration fields in the torch
 $(10 < d_p < 130 \mu\text{m}, m_C = 7.5 \text{ g/min})$

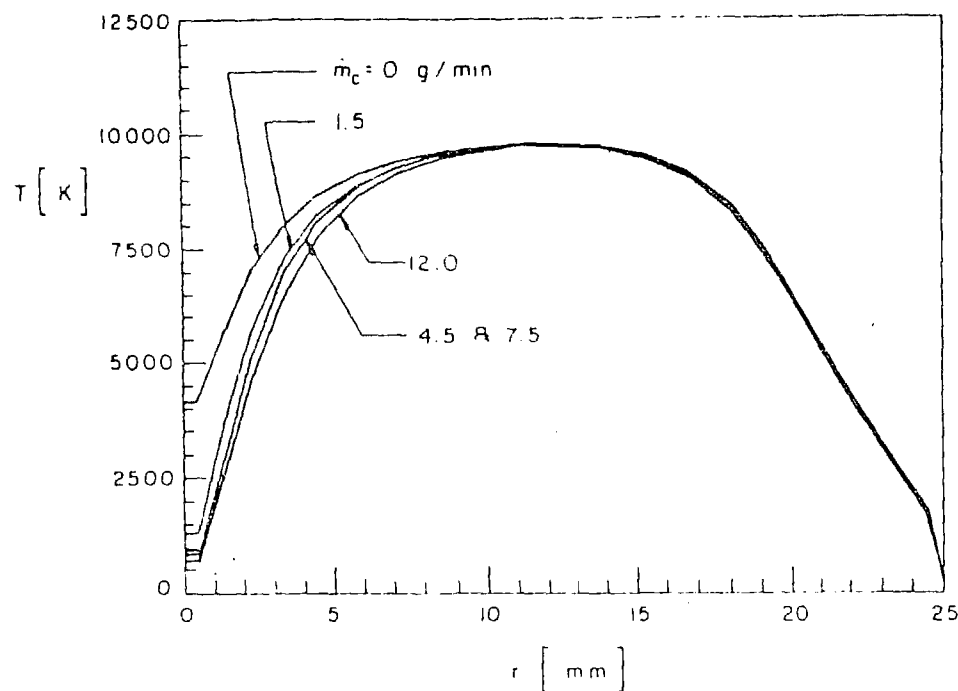


Figure 5. Radial temperature profiles in the middle of the coil for different copper powder injection rates ($10 \leq d_p \leq 130 \mu\text{m}$)

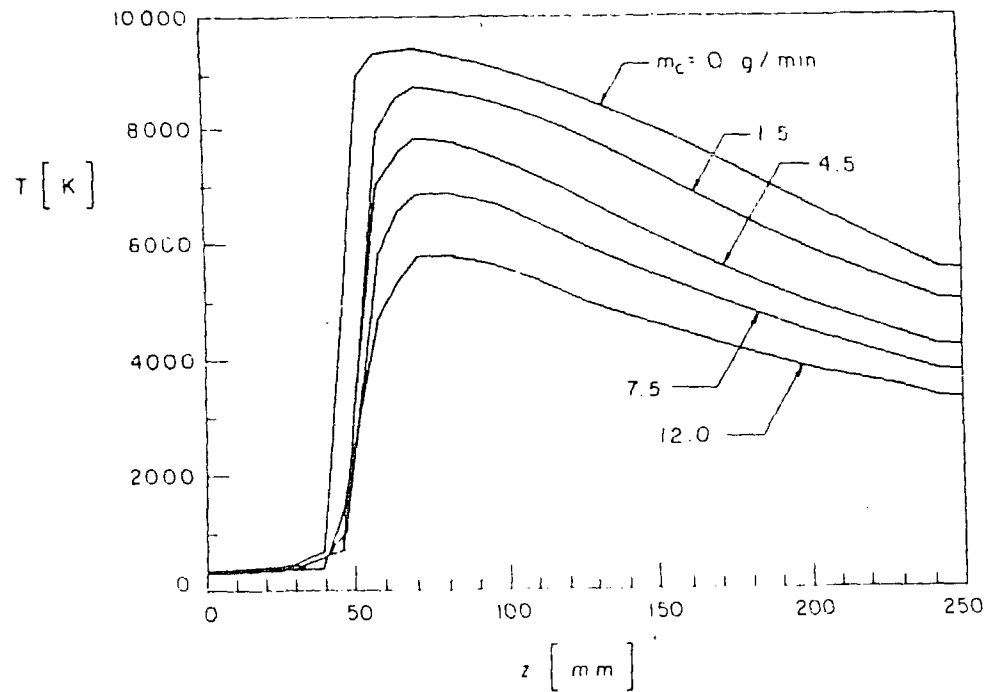


Figure 6. Temperature profiles along the axis of the torch for different copper powder injection rates ($10 \leq d_p \leq 130 \mu\text{m}$)

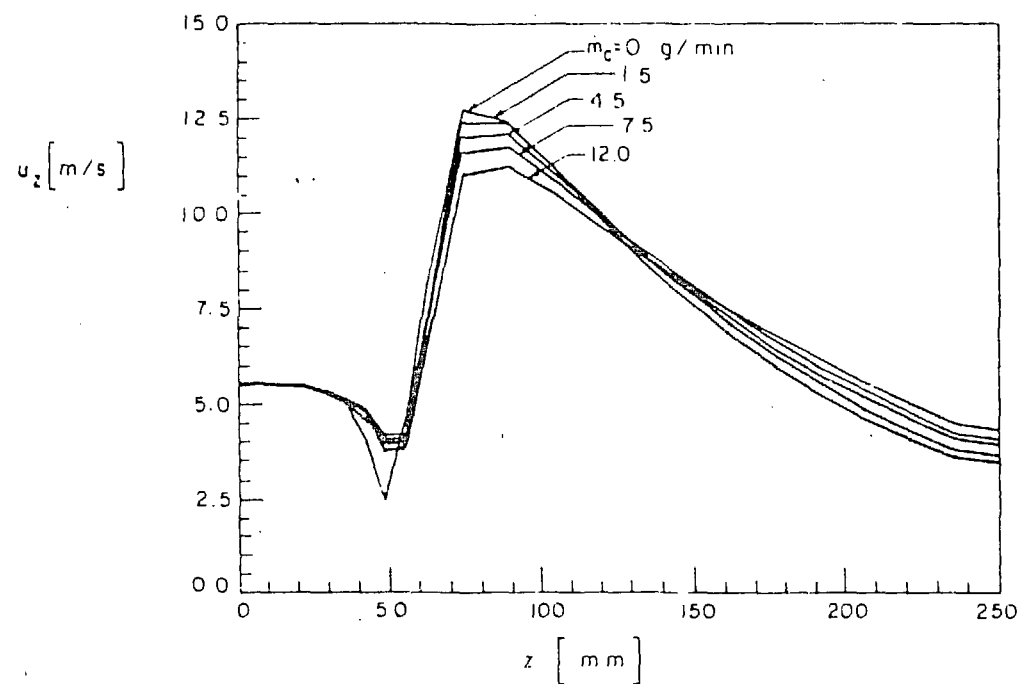


Figure 7. Axial velocity profiles along the axis of the torch for different copper powder injection rates ($10 \leq d_p \leq 130 \mu\text{m}$)

DISCLAIMER

This report was prepared as an account of work sponsored by an agency of the United States Government. Neither the United States Government nor any agency thereof, nor any of their employees, makes any warranty, express or implied, or assumes any legal liability or responsibility for the accuracy, completeness, or usefulness of any information, apparatus, product, or process disclosed, or represents that its use would not infringe privately owned rights. Reference herein to any specific commercial product, process, or service by trade name, trademark, manufacturer, or otherwise does not necessarily constitute or imply its endorsement, recommendation, or favoring by the United States Government or any agency thereof. The views and opinions of authors expressed herein do not necessarily state or reflect those of the United States Government or any agency thereof.